Towards Reconstructing Fingerprints From Minutiae Points

Arun Ross[a], Jidnya Shah[a] and Anil K. Jain[b]

[a] West Virginia University, Morgantown, WV, USA.
[b] Michigan State University, East Lansing, MI, USA.

ABSTRACT

We show that minutiae information can reveal substantial details such as the orientation field and the class of the associated fingerprint that can potentially be used to reconstruct the original fingerprint image. The proposed technique utilizes minutiae triplet information to estimate the orientation map of the parent fingerprint. The estimated orientation map is observed to be remarkably consistent with the underlying ridge flow. We next discuss a classification technique that utilizes minutiae information alone to infer the class of the fingerprint. Preliminary results indicate that the seemingly random minutiae distribution of a fingerprint can reveal important class information. Furthermore, contrary to what has been claimed by several minutiae-based fingerprint system vendors, we demonstrate that the minutiae template of a user may be used to reconstruct fingerprint images.

1. INTRODUCTION

Most biometric systems do not store the raw biometric data in its entirety but rather extract a salient set of features (known as a template) from the biometric data of a user. Since the template, by definition, is a compact description of the biometric sample, it is not expected to reveal significant information about the original data. Therefore, template-generation algorithms are typically assumed to be one-way algorithms. However, Adler[1] has demonstrated that a face image can be regenerated from a face template using a "Hill Climbing Attack". He employed an iterative scheme to reconstruct a face image using a face verification system that releases match scores. The algorithm first selects an estimate of the target face from a local database comprising of a few frontal images by observing the match score corresponding to each image. An eigen-face (computed from the local database) scaled by 6 different constants is added to this initial estimate resulting in a set of 6 modified face images which are then presented to the verification system. The image resulting in an improved match score is retained and this process is repeated in an iterative fashion. Within a few thousand iterations, an image that can successfully masquerade as the target face image is generated. The salient feature of this algorithm is that it does not require any knowledge of either the matching technique or the structure of the template used by the authentication system. The algorithm was successfully tested on 3 well known commercial face recognition systems. This type of *masquerade attack* can be easily extended to other biometric modalities as illustrated by Hill[2] who proposed a method for creating a digital fingerprint artefact from a minutiae template. Hill also devised a simple scheme to predict the shape (class) of the fingerprint using the minutiae template.

In this work we develop a technique for reconstructing fingerprints using minutiae information alone. Our technique is significantly different from the one proposed by Hill both in its approach as well as its scope. We extract a set of features from the minutiae template in order to infer both *the orientation map and the class* of the associated fingerprint. We then use Gabor-like filters to reconstruct fingerprints using the orientation information. Experiments conducted on the NIST-4 database indicate the efficacy of the proposed algorithm and suggests its potential in providing insights into the nature of the minutiae distribution for different classes of fingerprint.

Further author information: (Send correspondence to A. Ross)

A. Ross: ross@csee.wvu.edu

J. Shah: jidnyas@csee.wvu.edu

A. K. Jain: jain@cse.msu.edu

1.1. Fingerprint minutiae

A fingerprint is a smoothly flowing pattern of alternating ridges and valleys. The ridges do not flow continuously but rather display various types of imperfections known as minutiae (minor details in fingerprints). At the time of enrollment in a fingerprint system, important minutiae information (typically, positions of ridge endings and bifurcations, and the associated orientations) is extracted and stored in the database in the form of a template. Fingerprint matching is accomplished by comparing the minutiae distribution of two fingerprints via sophisticated point pattern matching techniques.[3]

The ridge pattern in a fingerprint allows for a systematic classification procedure. According to the Galton-Henry classification scheme,[4] over 95% of fingerprints can be classified into five classes, viz., arch (**A**), tented arch (**T**), right loop (**R**), left loop (**L**) and whorl (**W**). Alternately, the **T** and **A** classes may be combined into one single class resulting in four classes. A visual glance at the minutiae plots of the four classes (Figure 1) suggests the possibility of deducing the fingerprint class from the minutiae points.
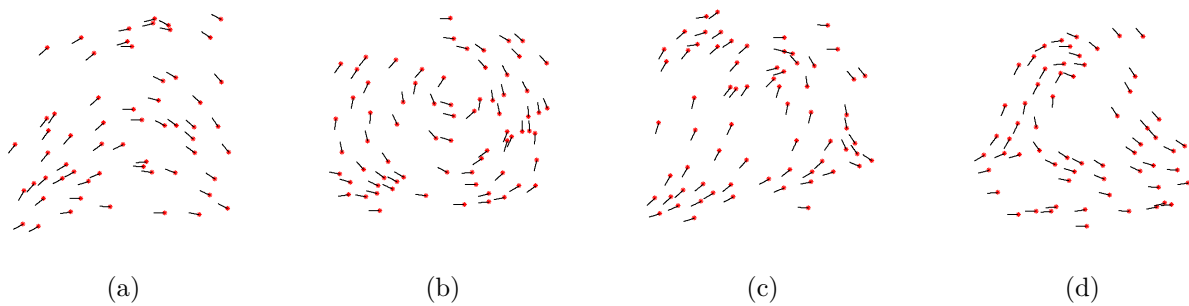

(a)   (b)   (c)   (d)

Figure 1. Minutiae distribution of 4 fingerprint classes: (a) **A**, (b) **W**, (c) **L**, and (d) **R**.

Minutiae have been studied extensively in the forensic literature specifically in the context of fingerprint individuality models.[5] For example, Galton[6] observed a strong correlation between the class of a fingerprint and the occurrence of a minutiae at a specific location in the image (Figure 2).
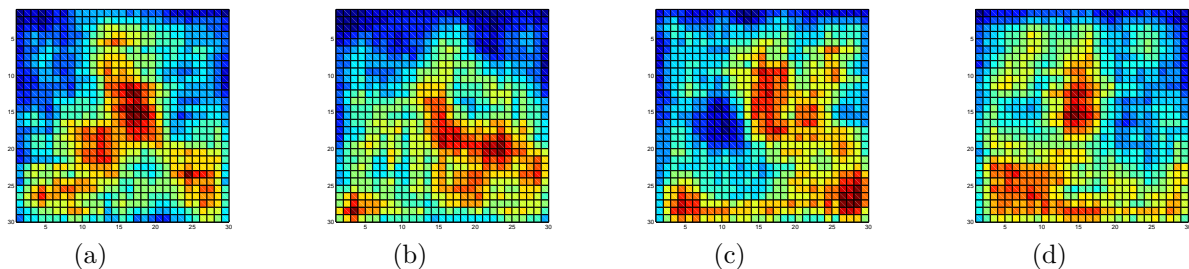

(a)   (b)   (c)   (d)

Figure 2. Minutiae density associated with 4 different classes of fingerprints: (a) A, (b) W, (c) L, and (d) R. These plots were generated using 30 images per class. Red (Blue) color indicates a high (low) density region.[7]

Typically, minutiae points have been used only for fingerprint alignment and matching. In this paper, we demonstrate that they can be used to estimate the orientations of the underlying ridge flow as well as to determine the class of the fingerprint. We also present initial results for the reconstruction of fingerprint images using the minutiae distribution. The rest of the paper is organized as follows: the algorithm for orientation prediction is described in section 2; the minutiae-based classification algorithm is explained in section 3; our algorithm for fingerprint reconstruction is discussed in section 4; section 5 provides future direction to this work.

2. PREDICTING RIDGE ORIENTATIONS USING MINUTIAE TRIPLETS

The orientation of a minutia is an indication of the local ridge direction since the fingerprint is a smoothly changing oriented texture pattern. Therefore, by observing the orientation of a group of minutiae one can 'interpolate' the underlying local ridge information. The proposed algorithm utilizes a set of three minutiae points (minutiae triplet) to predict the orientation of a triangular fingerprint region defined by the triplet. In our formulation, a minutia is represented as a three-tuple value, (x, y, θ), where (x, y) is its spatial location and θ is its orientation*. The algorithm for generating the orientation map has four main stages: (i) triplet generation; (ii) orientation prediction; (iii) triplet pruning; and (iv) orientation smoothing.

1. **Triplet generation** :

    Consider a minutiae template, $\mathcal{M}$, of a fingerprint containing N minutiae points given by, $\mathcal{M} = \{m_1, m_2, \cdots, m_N\}$ where $m_i = (x_i, y_i, \theta_i)$. A set of 3 minutiae points, $\{m_i\}_{i=1,2,3}$, characterized by a triangle with sides $\{L_i\}_{i=1,2,3}$ and interior angles $\{\phi_i\}_{i=1,2,3}$ is said to constitute a 'valid' triplet, T, if the following conditions hold.

    (a) $L_{min} \leq L_i \leq L_{max}$, $\forall\ i = 1, 2, 3$. This ensures that the perimeter of the triangle traverses a compact region, thus, avoiding the large global variability observed in the fingerprints of most classes.

    (b) $\theta_{dif} \leq \theta_{tol}$, where $\theta_{dif} = \max_{i=1,2,3}(\theta_i - \theta_{med})$ and θ_{med} is the median of $\{\theta_i\}_{i=1,2,3}$. This ensures that the orientations of component minutiae points are within a small interval.

    (c) $\phi_i > \phi_{min}$, $\forall\ i = 1, 2, 3$. This ensures that "narrow" triangles subtending a very small area are avoided.

    In our experiments using the NIST-4 database the following values were used: $L_{min} = 20$, $L_{max} = 300$, $\theta_{tol} = 30^o$ and $\phi_{min} = 20^o$.

2. **Orientation prediction** : Consider a pixel $P(x, y)$ located inside the triangular region defined by the triplet, T. Let $d_i = dist\{m_i, P\}$, $i = 1, 2, 3$, be the Euclidean distance of this pixel from all the three vertices such that $d_1 < d_2 < d_3$. The orientation of the pixel, $O(x, y)$, is then computed as,

$$O(x,y) = \frac{d_3}{(d_1 + d_2 + d_3)}\theta_1 + \frac{d_2}{(d_1 + d_2 + d_3)}\theta_2 + \frac{d_1}{(d_1 + d_2 + d_3)}\theta_3. \tag{1}$$

    The angle θ_1 (θ_3) corresponds to the orientation of the vertex that is nearest to (farthest from) the pixel $P(x, y)$. Thus, $O(x, y)$ is computed as a weighted sum of all the three orientations with a higher weight being assigned to the orientation of the closest vertex. The generated orientation map is shown in figure 3. The orientations of ridges and, thus, of associated minutiae in whorls change rapidly over a small area (e.g. at the core region). Therefore, if triplets covering a large area are selected in the case of whorls, then an accurate prediction may not be rendered. However, in the case of arches, larger triplets provide good results since such rapid variations are not observed. The triplet generation procedure described above is more conservative and is observed to work well for all classes of fingerprints.

3. **Triplet pruning** : In a fingerprint image, minutiae tend to appear in clusters.[8] For instance, the regions near the core and delta have dense minutiae activity. It is therefore possible for a triplet to reside inside the triangular region of another triplet or overlap with it. In such cases, rather than consolidating the orientation information predicted by multiple triplets, we utilize the information predicted only by a single good quality triplet. The quality, Q, of each selected triplet is measured by examining the average length of the sides of the triangle (L_{avg}), the orientations of component minutiae points with respect to the median (θ_{diff}), and is computed as,

$$Q = (L_{max} - L_{avg})\,w_1 + \left(\frac{\theta_{tol} - \theta_{dif}}{\theta_{dif}}L_{max}\right)w_2. \tag{2}$$

---

*For orientation prediction we do not make a distinction between opposing angles, i.e., both 30° and 150° orientations are assumed to be the same.

(a)   (b)   (c)
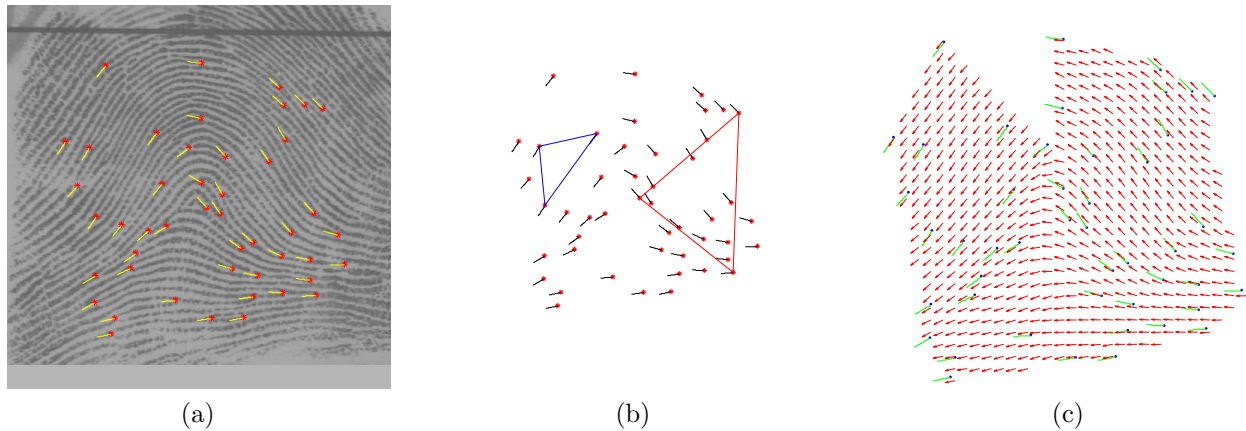
Figure 3. (a) Minutiae distribution of a fingerprint. (b) Examples of a good quality triplet (blue) with $L_{avg} = 112.66$, $\theta_{diff} = 5$, $Q = 237.63$ and a bad quality triplet (red) with $L_{avg} = 217$, $\theta_{diff} = 26$, $Q = 67.55$. (c) Estimated orientation map.

Here, w_1 and w_2 are the weights associated with each term ($w_1 = 0.4$ and $w_2 = 0.6$, in our experiments). This ensures that a triplet having minutiae of similar orientations and traversing a relatively compact region is assigned a higher Q value (Figure 3(b)). A good quality triangle will lead to a better estimation of the orientation of the underlying ridges according to our algorithm. We compute the orientation at discrete points (every 13th pixel) in the fingerprint region. Hence, for a 512×512 image, a 39×39 orientation map is generated.

4. **Averaging the orientation map**: To obtain a smooth transition in orientations, the predicted orientation map is convolved with a 3×3 local averaging filter.

3. CLASSIFICATION OF FINGERPRINTS USING MINUTIAE FEATURES

Fingerprint classification refers to the problem of assigning a fingerprint to a pre-defined class in a consistent and reliable way. Usually fingerprint matching is performed using local features such as local ridge and minutiae details whereas fingerprint classification uses global features such as the ridge shape and singular points. All existing fingerprint classification schemes use the fingerprint image along with one or more features like ridge line flow, location of singularities, or the orientation map to determine the fingerprint class. A detailed literature review of existing fingerprint classification techniques is described by Maio et al.[9]

In this paper, we use only the minutiae information for classification. Roxburgh[10] observed a correlation between neighboring minutiae and variation in minutiae position with the pattern of the fingerprint. Such observations reported in the forensic literature substantiate our hypothesis that the seemingly random distribution of minutiae in a fingerprint can reveal important information about the class of a fingerprint. The main steps of our minutiae-based classification algorithm are summarized in the block diagram shown in Figure 4.
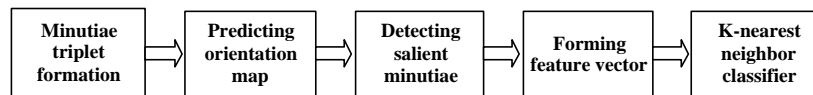

Figure 4. The minutiae-based classification algorithm.

1. **Detecting registration point using Hough Transform** : A visual analysis of the fingerprint ridge patterns of various classes indicates that they all have almost the same ridge structure in the base and marginal areas[11] as shown in Figure 5.
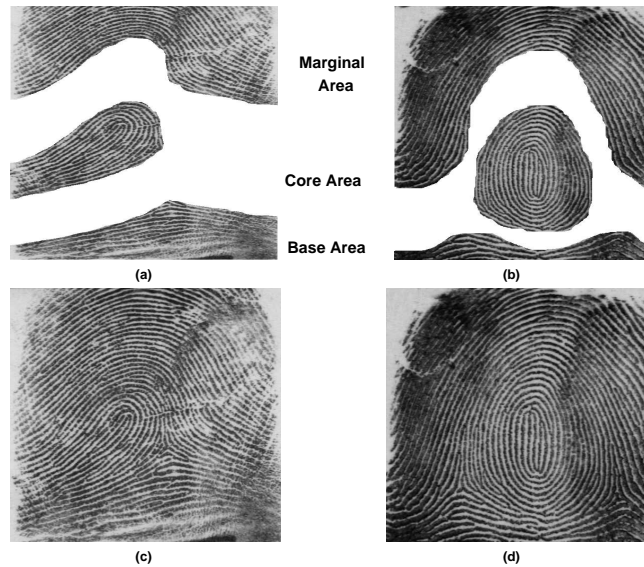
Figure 5. (a) and (b) show the base, core and marginal area of two fingerprints representing the L and W classes. (c) and (d) are the corresponding original fingerprints.

But the irregularities in the vicinity of the core (such as a circular ridge pattern in the case of whorls or the recurving of ridges in the case of loops) are significant from a classification standpoint. Therefore, the minutiae present in the vicinity of core point can reveal important class characteristics. In order to select these 'salient' minutiae, we first detect a registration point (R_0) using the Hough transform[12] which can identify parametric shapes when sufficient evidence is available. In our case, this evidence consists of minutiae coordinates and their orientations. We specifically observe that the ridges around the core point exhibit high curvature forming a nearly circular pattern and, consequently, the *orientations* of minutiae associated with these ridges may aid in the detection of the registration point.

Note that all minutiae contributing to a potential circle will have orientations almost tangential to the circumference. Figure 6(a) shows an ideal plot of minutiae residing on the circumferences of two concentric circles. Since the minutiae orientation is perpendicular to the radius joining the minutiae and the center point, each minutiae m can define a set of circles whose centers lie on the line L that is perpendicular to the orientation of m (Figure 6(b)). The radius r of each circle is the distance between m and the corresponding center. Thus, a 3D accumulator in Hough space denoted as (x, y, r) can be used for detecting R_0 as described below.

(a) Initialize the accumulator $A(x, y, r)$ where (x, y) is the center of the potential circle with radius r.

(b) For each minutiae m_i, $i = 1$ to N, the potential centers (x, y) lie on the line L. The accumulator cell $A(x, y, r)$ is incremented if the point (x, y) is at a distance r from minutiae m_i.

(c) For a circular minutiae pattern, there will be a well-pronounced peak in the Hough parameter space corresponding to one center (x, y). This is the registration point, R_0, that is characterized by significant minutiae activity around it.

We use both the minutiae information and the predicted orientation map to detect the registration point. Since the ridge structure in fingerprints is not circular, we also consider lines that are nearly perpendicular ($\pm 30^o$) to the orientation θ. The results of the Hough Transform using the predicted orientation maps of various classes are shown in Figure 7. Note that in all cases R_0 is detected in the vicinity of the true 'core' or 'center' point.
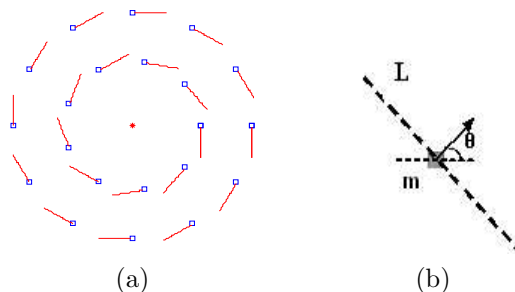
(a)   (b)

Figure 6. Using the Hough transform to detect the registration point. (a) An ideal minutiae distribution defining the center of a circle ('*'). (b) Line L is perpendicular to the orientation (θ) of minutiae m. Each point on L represents the center of a potential circle.

2. **Selecting salient minutiae** : As stated earlier, the minutiae in the vicinity of the core region have class-representative properties. Thus only the minutiae located in a 300×300 region about R_0 are used by the classification algorithm (Figure 8).

3. **Generating feature vectors** : We next extract a set of 11 features from the minutiae distribution. Most of these class-representative minutiae characteristics have been studied by various forensic experts such as Galton,[6] Roxburgh[10] and Kingston[8] in the context of fingerprint individuality; however, these have not been used for classifying fingerprints. Our goal is to imitate the procedure adopted by a human fingerprint expert instructed with the task of classifying fingerprints using minutiae information alone. Features such as minutiae density and clusters of minutiae having homogeneous orientations are easily captured by the human eye but pose a significant challenge to machine vision systems.

The features we use are invariant to rotation and translation of the parent fingerprint image. The 11-dimensional vector $F = \{F_1, F_2, \cdots, F_{11}\}$ is constructed as follows.

(a) **Features based on minutiae orientations (F_1, F_2)** : The direction of ridge flow varies from one class to another and so does the minutiae orientation. For instance, the **W** class has at least one ridge which traces a 360 degree closed path in the central region of the fingerprint. Thus the orientations of these minutiae range from $0 - 360$ degrees. On the other hand, the minutiae orientations of **A** have only two dominant directions. In order to understand the distribution of minutiae orientations for each class, we examine the rose plots † of minutiae orientations (Figure 9). One feature capturing these variations in minutiae orientations across classes is the *number* of empty bins in the rose plot (F_1). This indirectly captures the spread of minutiae orientations. Also, F_2 is defined to be the variance in the orientations of the minutiae points.

(b) **Features relating minutiae pairs $(F_3, \cdots, F_6)$** : Minutiae pairs are fundamental units for representing variations in fingerprints[13] since the properties of neighboring minutiae vary with fingerprint class. For instance, the neighboring minutiae in the central region of **W** have large orientation differences whereas minutiae neighbors in class **A** have similar orientations. The correlation between spatial location and orientations of minutiae pairs can be examined by estimating the joint distribution $P(R, \Phi)$, where R is the distance between two minutiae and Φ is the difference in their orientation. Six different features (see Eqns. (3) - (6)) are extracted from this joint distribution. F_3 represents minutiae pairs that are spatially close to each other and have almost similar orientations, while F_4 represents pairs that are close but have a large orientation difference. F_5 represents minutiae pairs that are far away from each other and having similar orientations, and F_6 represents minutiae pairs that are far away from each other but having large orientation differences.

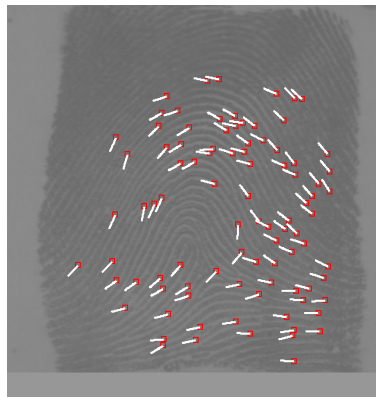$$F_3 = \sum_{0 \leq R \leq R_1} \sum_{0 \leq \Phi \leq \Phi_1} P(R, \Phi) \, dR \, d\Phi, \qquad (3)$$

---

†The rose plot is a a polar plot showing the histogram of angles.
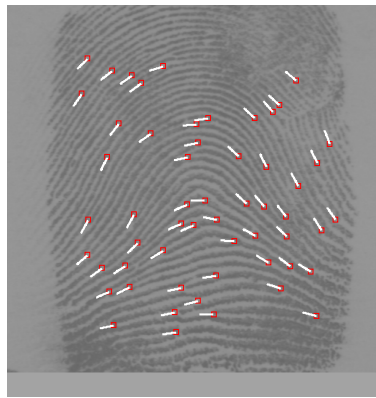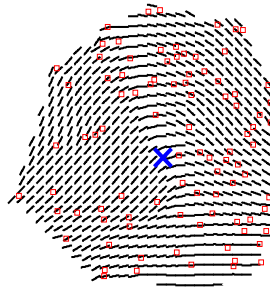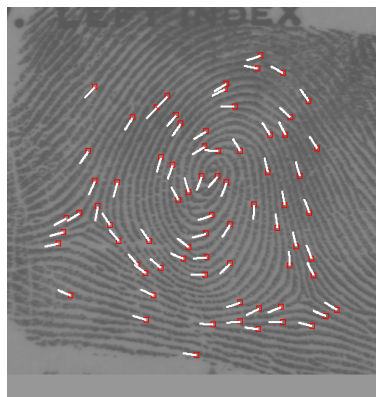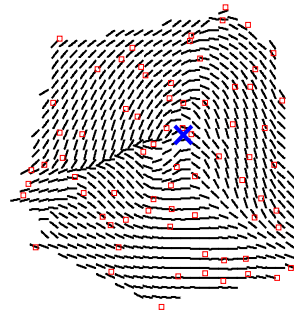
(a)
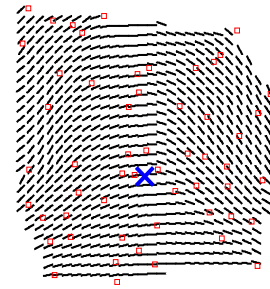
(b)

(c)

(d)

(e)

(f)

Figure 7. (a), (c), (e) show the minutiae distribution of three classes (**A**, **L** and **W**). The corresponding R_0 points ('X') detected using the estimated orientation maps are shown in (b), (d) and (f).
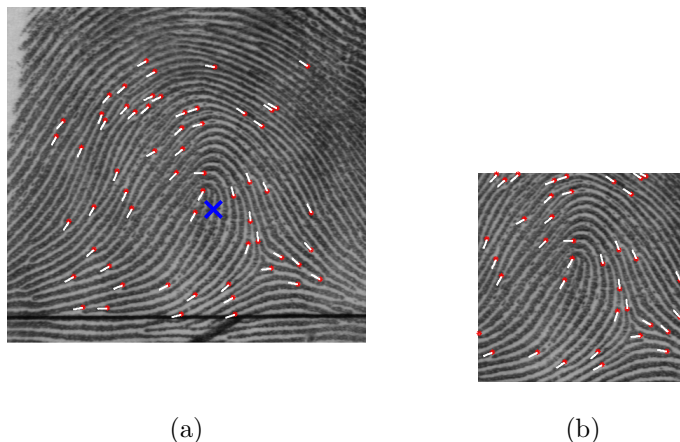
(a)   (b)

Figure 8. (a) The minutiae distribution of a fingerprint image along with the detected registration point, R_0 ('X'). (b) The salient minutiae in a 300×300 region about R_0.

$$F_4 = \sum_{0 \leq R \leq R_1} \sum_{\Phi_1 \leq \Phi \leq \Phi_2} P(R, \Phi)\, dR\, d\Phi, \tag{4}$$

$$F_5 = \sum_{R \geq R_2} \sum_{0 \leq \Phi \leq \Phi_1} P(R, \Phi)\, dR\, d\Phi, \tag{5}$$

$$F_6 = \sum_{R \geq R_2} \sum_{\Phi_1 \leq \Phi \leq \Phi_2} P(R, \Phi)\, dR\, d\Phi. \tag{6}$$

In our experiments, $R_1 = 60$, $R_2 = 180$, $\Phi_1 = 30^o$ and $\Phi_2 = 180^o$. It is observed that these distributions are significantly different across the four fingerprint classes. The above probabilities can be computed by finding the number of minutiae pairs satisfying the above mentioned criteria for R and Φ divided by the total number of minutiae pairs.

(c) **Features representing clustering of minutiae** (F_7, F_8) : Minutiae have a tendency to cluster in certain regions of a fingerprint. Kingston estimated the probability of observing a particular number of minutiae from the minutiae density by assuming a Poisson distribution.[8] Whorls are characterized by high minutiae density near the core region. Champod and Margot observed that such high density regions vary from one fingerprint class to another.[14] F_7 is the maximum minutiae density observed in a local area (i.e., a circle of radius 50) of the fingerprint. This value is relatively high for **W** and low for **A**. The feature F_8 is the maximum variance in minutiae orientations of a minutiae cluster within this radius.

(d) **Features capturing global ridge information** (F_9, F_{10}, F_{11}) : Visually it is apparent that features $F_1 \cdots F_8$ can distinguish classes **A** and **W**, but are not sufficient for distinguishing between the other classes (see Figure 1). It is, therefore, necessary to augment information about the global ridge pattern with the local minutiae properties. To capture the global ridge structure of the fingerprint, we define geometric kernels which model the shape of the fingerprint around the core region for the **W**, **L** and **R** classes. In a left loop, the ridges in the core region form a loop by recurving to the left side of the fingerprint. This is captured by a kernel formed using two semi-ellipses corresponding to the concave and convex parts of the loop. The kernel for **R** is a mirror image of the **L** kernel. The circular ridge structure of **W** is represented using a simple circle (Figure 10).
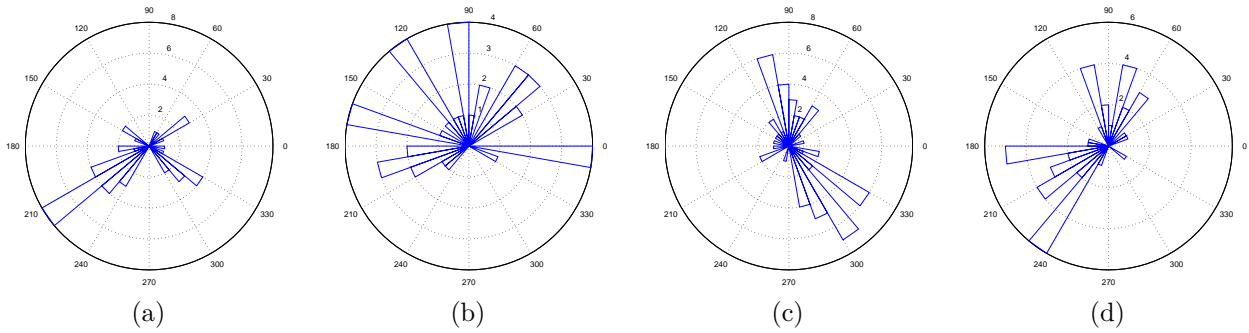
(a)   (b)   (c)   (d)

Figure 9. Rose plots of (a) **A**, (b) **W**, (c) **L**, (d) **R** fingerprint classes.

Since arch-like characteristics are observed in the marginal area of all classes of fingerprints (Figure 5), we do not define a kernel for class **A** as it would erroneously fit all the other classes. The kernel fitting algorithm that we have adopted is similar to the one proposed by Jain and Minut[15] for fingerprint classification and is based on the estimated orientation map. Consider V to be a smooth flow field (i.e., the orientation map) defined over some region in the plane R^2 and let β be its orientation. Let $\gamma_t = (x(t), y(t))$ be the kernel curve in R^2 as shown in Figure 11.
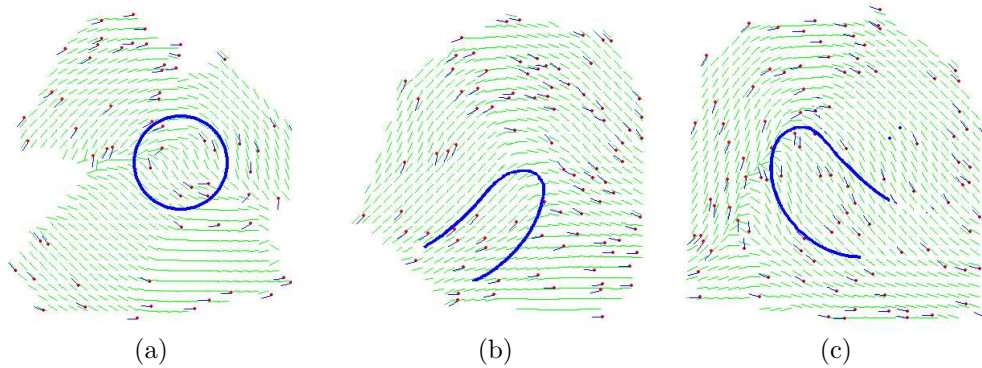

(a)   (b)   (c)

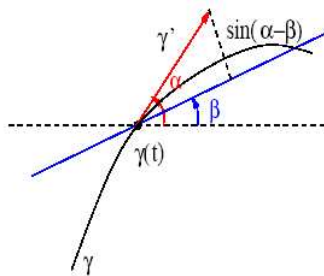**Figure 10.** Kernels for the (a) **W**, (b) **L** and (c) **R** classes.

Figure 11. The kernel fitting process. The red line is the unit tangent vector to the kernel while the blue line indicates the direction of flow field at point γ_t.[15]

Let $\dot{\gamma}$ be the tangent to γ and let α be its orientation. To find how well each kernel fits the orientation

map of the fingerprint, an energy functional capturing the difference between the direction of $\dot{\gamma}$ and that of the vector field V at point γ_t is defined as follows:

$$E(\gamma) = \frac{\int_{\gamma} sin^2(\alpha - \beta(\gamma)) \, d\gamma}{\int_{\gamma} d\gamma}. \tag{7}$$

The kernel-fitting process now becomes a simple energy minimization problem. For each predicted orientation map, we find three energy functional values (Eqn. 7) corresponding to the **L**, **R**, and **W** kernels. This results in features F_9, F_{10} and F_{11}, respectively. We observe that due to the inherent similarity in the ridge structures of the 2 loops and **A**, both the **L** and **R** kernels fit well for **A**. Therefore, for class **A** the values for F_9 and F_{10} will be very similar. This property is useful in resolving the ambiguity between the loops and class **A**. Note that the kernels are defined with respect to R_0; for **W**, R_0 is the center of the circle whereas for **L** and **R**, it is the focus of the elliptical kernel.

The rotation and translation of fingerprints are taken into account by subjecting these kernels to various types of transformations: the radius of the **W** kernel is varied in the interval $[100, 160]$; the semi-major axis of the **L** and **R** classes is varied in the interval $[120, 180]$ while the semi-minor axis is varied in the interval $[60, 100]$; the angle that the ellipse makes with the horizontal is varied in the range $[-10^o, 10^o]$. Further, the kernels themselves are translated in a 20×20 window around R_0. Only the minimum of each energy functional over all possible kernel transformations is used to define the features F_9, F_{10} and F_{11}.

4. **Classification of fingerprints** : The 5 nearest neighbor classifier ($5NN$) using the Manhattan distance was employed to classify the 11-dimensional feature. We conducted experiments using the NIST-4 database that contains 2000 pairs of fingerprint images (each of size 512×512) corresponding to five classes. Minutiae information was extracted using the algorithm proposed by Hong et al.[3] We combine the fingerprint templates from the **A** and **T** classes into one single class (**A**). Since we require a sufficient number of minutiae triplets to estimate the orientation map, we reject those templates having fewer than 25 minutiae points; also, the templates of ambiguous fingerprints (those having multiple class labels) were not considered. In order to ensure that we have the same number of samples per class, we eventually worked with 700 fingerprints from each class - 150 fingerprint templates (randomly chosen) were used for training and 550 templates were used for testing. We observe that by reducing the dimensionality of the feature vector from 11 to 8 via an exhaustive feature selection process (features F_5, F_6 and F_8 are eliminated) improves classification performance. The performance can be further improved by using the *weighted* manhattan distance where each feature is assigned a different weight based on its *individual* performance using the $5NN$ classifier. A classification rate of 82% was obtained and the resultant confusion matrix is shown in Table 1.

True Class	Assigned Class			
	A	**L**	**R**	**W**
A	467	45	32	6
L	61	464	7	18
R	69	26	448	7
W	4	61	68	417

Table 1. Confusion matrix indicating classification performance.

3.1. Analyzing classifier performance

Although our classification result is inferior to the present state-of-the-art fingerprint classification techniques,[9] our intention is to show that it is feasible to estimate the class of a fingerprint using its minutiae template alone. Most of the misclassifications represents the cases where ridges contributing to important pattern characteristics (e.g., recurring ridges) do not have minutiae. For example, in Figure 12 it can be seen that the minutiae plot does not capture the recurving of ridges in the core region of a right loop thus resulting in a classification error.
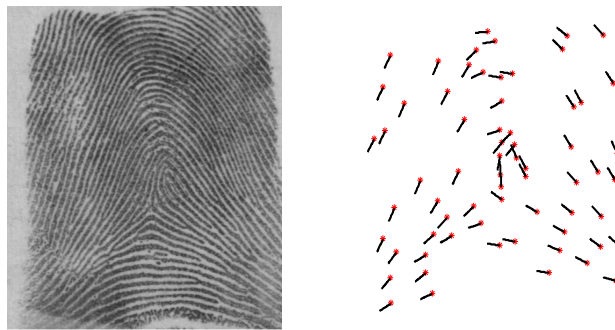
Figure 12. The minutiae distribution of a **R** class fingerprint. The recurving ridge information is not captured by the minutiae.

4. FINGERPRINT RECONSTRUCTION

Very few studies on synthetic fingerprint generation have been reported in the literature. The software developed by Cappelli et al.[16] called SFINGE uses Gabor-like space invariant filters to create fingerprint images. The SFINGE algorithm uses an iterative procedure to generate ridge patterns from an initially empty image containing a few seeds. In this process, fingerprint minutiae of different types are automatically generated at random positions.

In our reconstruction algorithm, we use the Gabor-like filter used by SFINGE. The filter, f, is the product of a cosine plane wave modulated by a Gaussian envelope, and takes the following form:

$$f(\mathbf{v}) = \frac{1}{\sigma^2} \, e^{-\frac{||\mathbf{v}||^2}{2\sigma^2}} \, [\cos(\mathbf{k}.\mathbf{v}) - e^{-\frac{\sigma||\mathbf{k}||^2}{2}}]. \tag{8}$$

Here, $\sigma = 1.2$ is the variance of the Gaussian envelope which decides the bandwidth of the filter, and $\mathbf{k}$ is the wave factor of the plane wave which is determined by the local (estimated) orientation. Let $\mathbf{z}$ be a point in the image about which the filter has to be applied. Further, let $O(\mathbf{z})$ denote the local estimated orientation. Then $\mathbf{k} = [k_x, k_y]$ can be derived by solving the following two equations:

$$D_{\mathbf{z}} = \sqrt{k_x^2 + k_y^2} \tag{9}$$

$$\tan(O(\mathbf{z})) = -\frac{k_x}{k_y} \tag{10}$$

$D(\mathbf{z})$ is related to the frequency of the filter and is set to $1/\sigma$. Our algorithm for fingerprint reconstruction is as follows. We divide an (empty) fingerprint image of size 512×512 into non-overlapping blocks. We then associate each block, $X_z^{(0)}$, with an orientation value, $O(\mathbf{z})$, estimated using our algorithm. Note that certain blocks may not have orientation information since the estimated orientation map can be incomplete. The block $X_z^{(0)}$ is next initialized with a noisy blob and is convolved with the filter, f, whose parameters are tuned using $O(\mathbf{z})$. This results in a new image $X_z^{(1)}$ which is again subjected to the convolution procedure; this process is repeated k times resulting in an image $X_z^{(k)}$ which exhibits ridge-like patterns. Figure 13 shows the ridge pattern generated over the entire fingerprint region ($k = 25$). Since a constant value of $\sigma = 1.2$ is used for all the blocks, the inter-ridge spacing is observed to be the same throughout the image. This algorithm gives good reconstruction results for all the fingerprint classes.
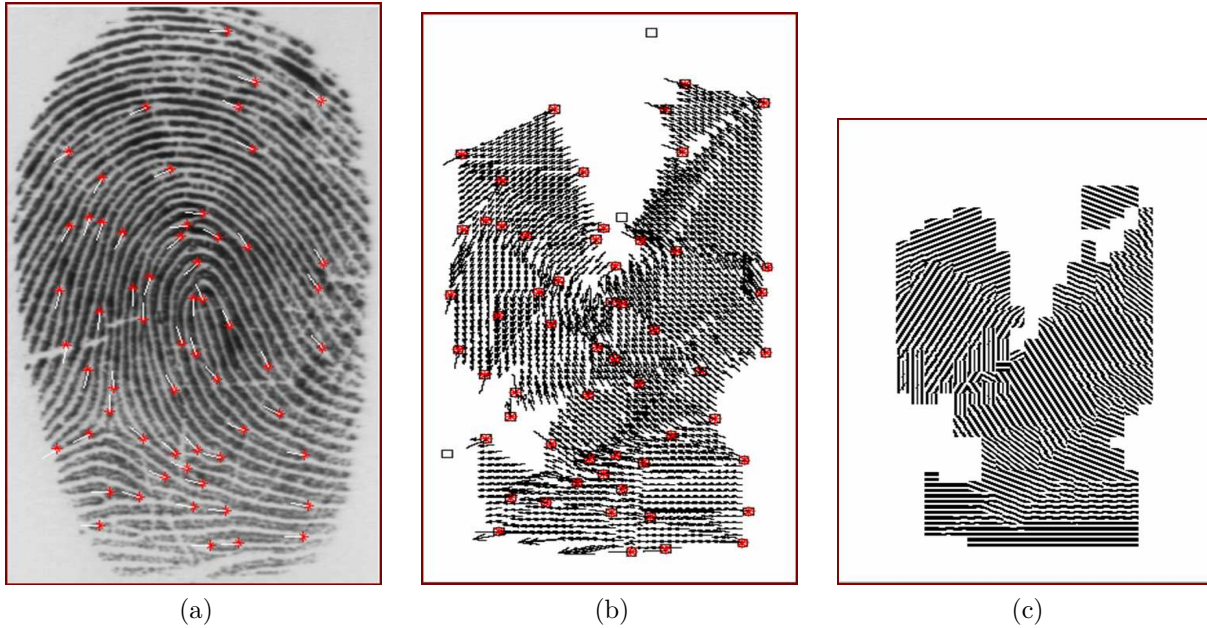
Figure 13. Reconstructing fingerprints. (a) Minutiae distribution of a fingerprint image. (b) Predicted orientation map (c) Reconstructed fingerprint.

5. SUMMARY AND FUTURE WORK

We have shown that the orientations of fingerprint ridges can be effectively predicted using minutiae points. This can be beneficial in applications like smart cards (where memory is critical) since the orientation map required for matching need not be stored explicitly but can be generated from the template. We have also demonstrated that minutiae information alone may be used for classifying fingerprints. We are currently exploring the use of a hierarchical classifier to perform classification.

Vendors of several minutiae-based fingerprint systems have denied the possibility that the stored templates could be used to generate implicit fingerprint information.[‡] Our preliminary results on reconstruction show that minutiae templates are indeed vulnerable to the masquerade attack. The increasing use of biometric systems with vulnerable templates demands the design of robust fingerprint templates (besides employing encryption, watermarking and shielding functions[17]). One potential approach would be to systematically *exclude* certain salient minutiae from the template that are critical to image reconstruction without drastically affecting the matching performance. We are also looking at ways to reconstruct the fingerprint image with the minutiae placed at pre-determined locations. Finally, a way to exploit the predicted class information for reconstruction needs to be explored.

6. ACKNOWLEDGEMENTS

[‡]All web-sites last accessed in January 2005:

1. http://www.biometricaccess.com/company/n_050798.htm: "You cannot reconstruct the original image from the minutiae..."

2. http://www.dodgeglobe.com/stories/111100/bus_scans.shtml: "...template of minutiae points cannot be used to re-create the original fingerprint..."

3. http://www.sun.com/solutions/documents/white-papers/SNAP_SolutionsGuide.pdf: "..it is not possible to recreate the fingerprint from the stored template.."

REFERENCES

1. A. Adler, "Can images be regenerated from biometric templates?," in *Biometrics Consortium Conference*, (Arlington, VA), September 2003.

2. C. Hill, "Risk of masquerade arising from the storage of biometrics," Master's thesis, Australian National University, 2001.

3. A. K. Jain, L. Hong, and R. Bolle, "On-line fingerprint verification," *IEEE Trans on Pattern Analysis Machine Intelligence* **19**, pp. 302–314, April 1997.

4. E. Henry, *Classification and Uses of fingerprints*, Routledge, London, 1900.

5. S. Pankanti, S. Prabhakar, and A. K. Jain, "On the individuality of fingerprints," *IEEE Transactions on Pattern Analysis and Machine Intelligence* **24**(8), pp. 1010–1025, 2002.

6. F. Galton, *Finger Prints*, McMillan, London, 1892.

7. U. Uludag and A. K. Jain, "Fingerprint minutiae attack system," in *Biometrics Consortium Conference*, (Arlington, VA), September 2004.

8. C. Kingston, *Probabilistic Analysis of Partial Fingerprint Patterns*. PhD thesis, University of California, Berkeley, 1964.

9. D. Maltoni, D. Maio, A. K. Jain, and S. Prabhakar, *Handbook of fingerprint recognition*, Springer-Verlag, New York, Berlin Heidelberg, 1st ed., 2003.

10. T. Roxburgh, "On the evidential value of fingerprints," *Sankhya: Indian Journal of Statistics* , pp. 189–214, 1993.

11. C. V. K. Rao, *Pattern Recognition Techniques Applied to Fingerprints*. PhD thesis, Linkoeping, Sweden, 1977.

12. D. H. Ballard, "Generalizing the hough transform to detect arbitrary shapes," *Pattern recognition* **13**(3), pp. 111–112, 1997.

13. D. A. Stoney, *Quantitative Assessment of Fingerprint Individuality*. PhD thesis, University of California, Davis, 1985.

14. C. Champod and P. Margot, "Computer assisted analysis of minutiae occurrences on fingerprints," in *Proc. Int'l Symp. Fingerprint Detection and Identification*, p. 305, 1996.

15. A. K. Jain and S. Minut, "Hierarchical kernel fitting for fingerprint classification and alignment," in *Proc. of International Conference on Pattern Recognition*, **2**, pp. 469–473, August 2002.

16. R. Cappelli, D. Maio, and D. Maltoni, "Synthetic fingerprint image generation," in *Proc. of 15th Int. Conf. on Advances in Pattern Recognition*, **3**(5), pp. 475–478, 2000.

17. J.-P. Linnartz and P. Tuyls, "New shielding functions to enhance privacy and prevent misuse of biometric templates," in *Proc. of Audio- and Video-based Person Authentication*, pp. 393–402, (Guildford, UK), June 2003.